

TRIASSIC BRAIDED GRAVELLY RIVER  
DEPOSITS AT PT. LEPREAU  
NEW BRUNSWICK

By

GARY J. LOOSEMORE

A Thesis

Submitted to the Department of Geology  
in Fulfillment of the Requirements  
of Geology 4K6

McMaster University

April 1984

McMaster University  
Hamilton, Ontario

TITLE: Triassic Braided Gravelly River Deposits  
at Pt. Lepreau, New Brunswick

AUTHOR: Gary J. Loosemore

SUPERVISOR: Professor G.V. Middleton

NUMBER OF PAGES: ix, 70

### Abstract

A detailed section of the Duck Cove Member (Nadon, 1981) of the Triassic Lepreau Formation of Southern New Brunswick is measured.

The section consists of a complex sequence of conglomerates and sandstones with a minor occurrence of mudstones and breccia. A description of the facies is provided and an interpretation is based on observations of ancient and marine braided stream deposits of Miall (1978) and Allen (1983). The Markov chain analysis is used to describe the vertical succession of facies.

Paleoflow indicators suggest a flow towards the south or southeast. However this conclusion is based on limited availability of data.

### Acknowledgements

I wish to thank my supervisor, Dr. G.V. Middleton, for introducing me to the study area, and for discussions and suggestions during the year.

I would also like to thank Pedro Moreno H. for his assistance during the field work and for discussions during the write-up of this report. Thanks also to Randy Rice for the long discussions and encouragement during the data analysis and write-up. Financial assistance for field work was provided through a N.R.C. grant to Dr. Middleton.

Technical assistance in photography was provided by Jack Whorwood. In addition, thanks go to Carol Wagner for proof-reading the thesis and Madeline Loosemore for typing it.

## Table of Contents

### Chapter 1: Instruction:

1.1 purpose and Scope	Page 1
1.2 Location	1

### Chapter 2: Regional Geology and Stratigraphy:

2.1 Regional Geology	5
2.2 Stratigraphy	6
2.3 The Measured Section	8

### Chapter 3: Facies Description and Interpretation:

3.1 Introduction	13
3.2 Facies Description	13
3.2.1 Facies A	13
3.2.1.1 Introduction	13
3.2.1.2 Facies A <sub>1</sub>	15
3.2.1.3 Facies A <sub>2</sub>	18
3.2.1.4 Facies A <sub>3</sub>	18
3.2.1.5 Facies A <sub>4</sub>	19
3.2.2 Facies B	
3.2.2.1 Introduction	22
3.2.2.2 Facies B <sub>1</sub>	22
3.2.2.3 Facies B <sub>2</sub>	24
3.2.2.4 Facies B <sub>3</sub>	25

3.2.2.5 Facies B <sub>4</sub>	Page 25
3.2.2.6 Facies B <sub>5</sub>	27
3.2.2.7 Facies B <sub>6</sub>	27
3.2.3 Facies C	30
3.2.4 Facies D	30
3.3 Facies Interpretation	
3.3.1 Introduction	32
3.3.2 Facies A	33
3.3.2.1 Facies A <sub>1</sub>	33
3.3.2.2 Facies A <sub>2</sub>	33
3.3.2.3 Facies A <sub>3</sub>	34
3.3.2.4 Facies A <sub>4</sub>	34
3.3.3 Facies B	35
3.3.3.1 Facies B <sub>1</sub>	35
3.3.3.2 Facies B <sub>2</sub>	35
3.3.3.3 Facies B <sub>3</sub>	35
3.3.3.4 Facies B <sub>4</sub>	36
3.3.3.5 Facies B <sub>5</sub>	36
3.3.3.6 Facies B <sub>6</sub>	36
3.3.4 Facies C	37
3.3.5 Facies D	37
3.4 Summary	37

3.4.1 Introduction	Page 37
3.4.2 Markov Chain Analysis	39
3.4.3 Facies Assemblages	44
Chapter 4: <u>Paleocurrent:</u>	
4.1 Introduction	49
4.2 Method	50
4.3 Results	51
Chapter 5: <u>Conclusions:</u>	58
References	59
Appendix A	63
Appendix B	68

## List of Figures

1.1	Outcrop of the Lepreau Formation	Page 2
1.2	Overview of the measured section	4
2.1	Detailed measure section	12
3.1	Facies A <sub>1</sub>	17
3.2	Facies A <sub>1</sub>	17
3.3	Facies A <sub>2</sub>	20
3.4	Facies A <sub>3</sub>	20
3.5	Facies A <sub>4</sub>	21
3.6	Facies B <sub>1</sub>	26
3.7	Facies B <sub>4</sub>	26
3.8	Facies B <sub>4</sub>	28
3.9	Facies B <sub>5</sub>	28
3.10	Facies B <sub>5</sub>	29
3.11	Facies B <sub>6</sub>	29
3.12	Facies C	31
3.13	Facies D	31
3.14	Preferred facies relationship diagram	42
3.15	Succession cycles determined from the Markov chain analysis	46
4.1	Rose diagram plot for trough cross-beds	52
4.2	Rose diagram plot for planar tabular cross-beds	54
4.3	Rose diagram plot for curretn lineations	55

List of Tables

3.1	Main facies types	Page 14
3.2	Facies A subtypes	16
3.3	Facies B subtypes	23
3.4	Summary of facies code	38
3.5	Significant and Almost Significant transitions	45
3.6	Facies Assemblages	48

## Chapter 1

### Introduction

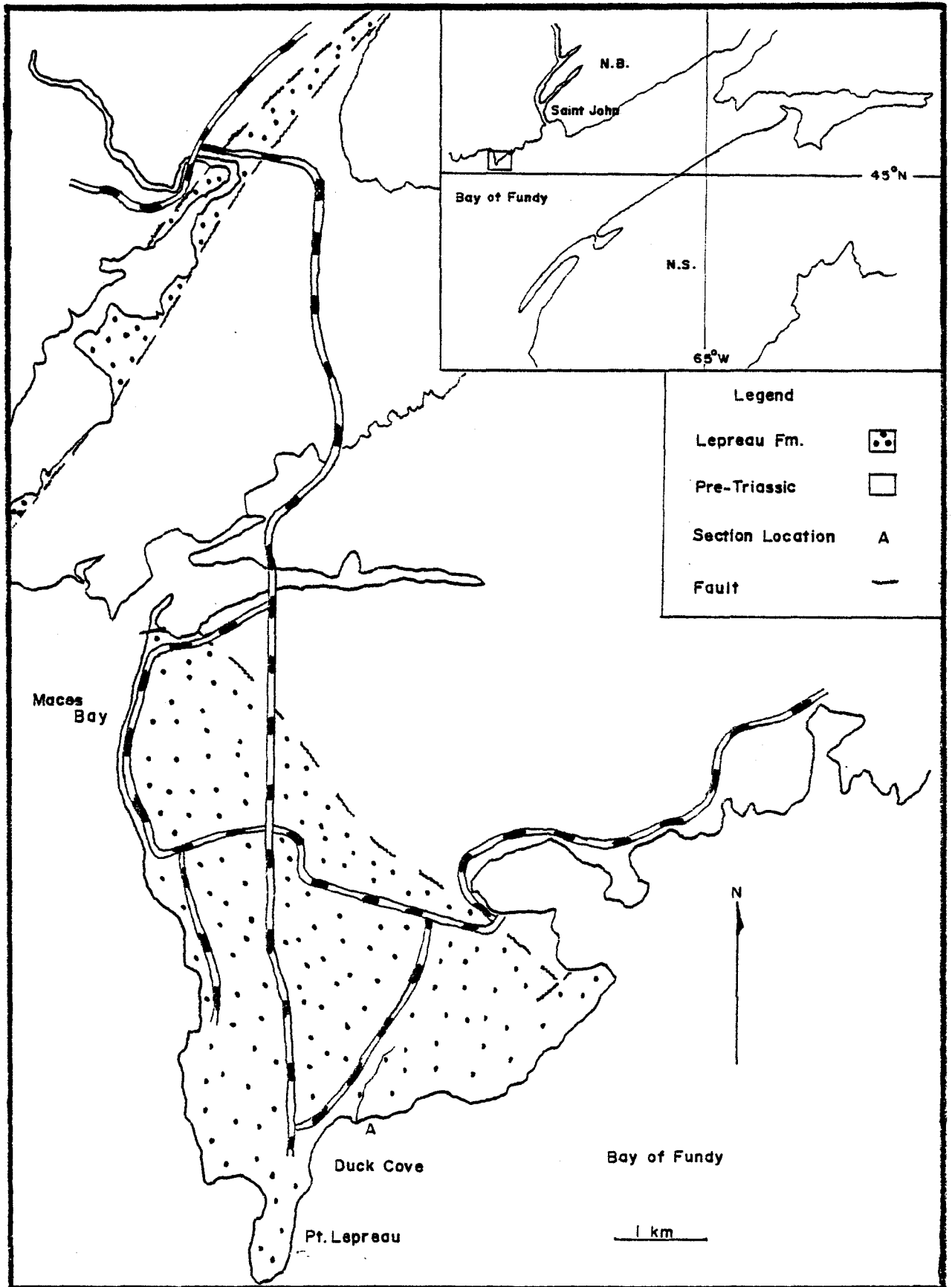
#### 1.1 Purpose and Scope

The purpose of this study is to describe and measure a detailed section of the Duck Cove Member of the Lepreau Formation of southern New Brunswick. The goal is to develop a facies description and to obtain paleocurrent data in order to better understand the environment of deposition.

#### 1.2 Location

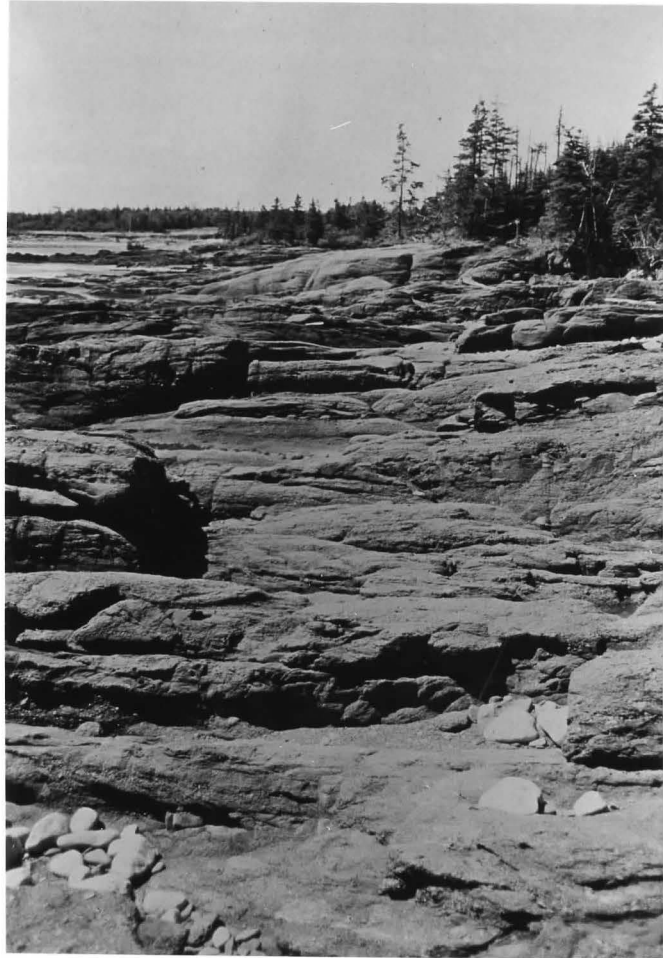
The measured section is located on Pt. Lepreau near the Pt. Lepreau Nuclear Generating Station, at approximately 66 27' longitude and 45 05' latitude. Outcropping on the northern shore of Duck Cove, the section can be reached by turning south off of Highway 1, 50 km west of Saint John on Highway 790 for 23 km, and then turning west following the sign for the Pt. Lepreau Nuclear Generating Station Information Centre. The nature trail leading from the information centre goes to Duck Cove and the top of the section is on the west bank of the small stream (Figure 1.1).

Figure 1.1. Outcrop of the Lepreau Formation based on  
Alcock (1945).



This particular section was chosen partly because of the ease of accessibility but more importantly, because its facies distribution typifies the lower part of the Duck Cove Member (Figure 1.2). Unfortunately, due to limited time for field work, a detailed section representing the top part of the member could not be measured and was only briefly examined.

Figure 1.2 Overview of the measured section at lowtide  
looking west. Trees for scale are approxi-  
mately 5 m high.



## Chapter 2

### Regional Geology and Stratigraphy

#### 2.1 Regional Geology

The Fundy Basin, into which the Lepreau Formation was deposited, has been described as a half-graben with the fault on the New Brunswick side of the basin (Swift and Lyall, 1968). In a half-graben basin, a greater thickness of section would be expected nearest the fault scarp, and a study by Klein (1962) confirmed this. The minimum stratigraphic thickness on the Nova Scotia side is reported as approximately 1060 m including the North Mountain Basalt which may be Jurassic in age. This measurement compares to the 2700 m thickness found at Pt. Lepreau and the 2200 m found at St. Martins (Nadon 1981).

The Fundy Basin is one of a series of basins along the eastern seaboard of the United States and Maritime Canada. Each basin shows a similar sequence of alluvial fan, fluvial and lacustrine sediments. There is however, no connection between the northeastern United States basins and the Fundy Basin because of doming of the crust between them (Le Pichon and Fox 1971).

## 2.2 Stratigraphy

Early work by Bailey and Mathews (1872) and Mathews (1896) indicated that the red beds outcropping along the coastal reaches of Pt. Lepreau, were of Carboniferous age. This conclusion was due to confusion with the Carboniferous Lancaster Formation which also contains abundant red beds and which outcrops near Pt. Lepreau. Belyea (1939) recognized a difference between the Pt. Lepreau rocks and the older Lancaster series and first named the rocks the Pt. Lepreau Formation.

After a name change to the Lepreau Formation by Wright and Clements (1943), Alcock (1945) mapped the Musquash area for the Geological Survey of Canada and included both the coastal section and a section outcropping along the Lepreau River as the Lepreau Formation. Alcock indicated that both sections are bounded by faults of unknown magnitude.

Klein (1962, 1963) investigated both the lithology and the paleocurrents of the coastal section and concluded that it was a mixture of low and high-rank greywackes, as well as arkoses. He determined that the formation had been derived from the south and could be roughly correlated

to the Triassic Formations at St. Martins.

The Lepreau River section has been dated by Sargeant and Stringer (1977) who have identified a reptile track called Isocampe lepreauense.

This track dates this portion of the formation as Middle to Upper Triassic. Unfortunately, the stratigraphic position of the Lepreau River section has not been determined with respect to the coastal section. Sargeant and Stringer (1977) report that the Lepreau River section consists of lithologies and structures similar to those of the coastal section, however, it has undergone a slightly different tectonic disturbance resulting in tighter folding.

Nadon (1981) briefly describes the Lepreau formation in his study on Triassic sedimentology of New Brunswick. He divided the coastal section into three members. The members, from the base of the formation upwards, are: the Fishing Point Member, the Duck Cove Member and the Maces Bay Member. However, Nadon did not examine the Lepreau River section.

The Fishing Point Member is composed of deep red breccias comprising various types of granites derived from a source to the east (Nadon 1981), interbedded with

rare, thin discontinuous fine sands and pebbly sandstones. The lower contact is not exposed, whereas the upper contact is erosional. The member is estimated from air photos to be approximately 350 m thick.

Nadon (1981) has interpreted this member to be a section deposited by debris flows on an alluvial fan, fining-upwards into the deposits of a playa-lake environment.

The Duck Cove Member, in which the measured section is located, consists of cross-bedded conglomerates interbedded with red shales and sandstones. The red colour is less strongly hued than in the lower Fishing Point Member, and the Duck Cove Member contains some grey-coloured beds. From air photos, the member is estimated to be approximately 1200 m thick and exhibits an overall fining-upward trend in grain size. The conglomerates are the dominant facies near the base of the member with little sandstone or shale. Further up, the shales and sandstones become more important in frequency and in quantity and, although still present, the conglomerates tend to be much sandier and have a much smaller clast size.

Near the top of the section, on the west side of the

point, the shales are very well-developed with moderately well-defined caliche horizons.

Nadon (1981) has interpreted the facies of this member to be representative of a braided river environment fining-upward into a floodplain sequence.

The lower contact of the Maces Bay Member has been set arbitrarily at the initial appearance of a clast-supported breccia, although otherwise the lower facies of the member is identical to that of the upper facies of the Duck Cove Member (Nadon 1981). Breccia increases in frequency in the member until near the top, where the breccias become very coarse and contain large boulders up to 2 m in size. This has been interpreted by Nadon (1981) as the deposits of debris flows. The member is estimated from air photos to be about 1200 m thick.

### 2.3 The Measured Section

The measured section is located stratigraphically approximately 250 m from the base of the Duck Cove Member. Bedding dips towards the northeast at approximately 30° and is interrupted locally by a system of joints or minor faults with an orientation of 060°.

The measured interval broadly mimics the overall fining-upward sequence exhibited by the member as a whole. Beginning with thick beds of clast-rich conglomerates at the base, there is an increase in frequency of sandstones and thinner, sandier conglomerates. Near the top of the section, the sandstones become finer and are thicker and more abundant than the conglomerates. Due to limited time, detailed work further up-section was not completed although a reconnaissance revealed a change to well-burrowed shales with occasional sandstones and rare conglomerates.

Accompanying this upward decrease in grain size, there is a change in scale and type of sedimentary structures. Near the base, the prominent structure is large-scale trough cross-bedded conglomerates with a high degree of lateral variability and erosional bases. Further up-section, the conglomerates are more abundantly planar bedded with smaller-scale trough cross-beds and planar cross-beds. The beds are generally thinner and show frequent lateral changes from planar-bedded to cross-bedded. Near the top, the prominent

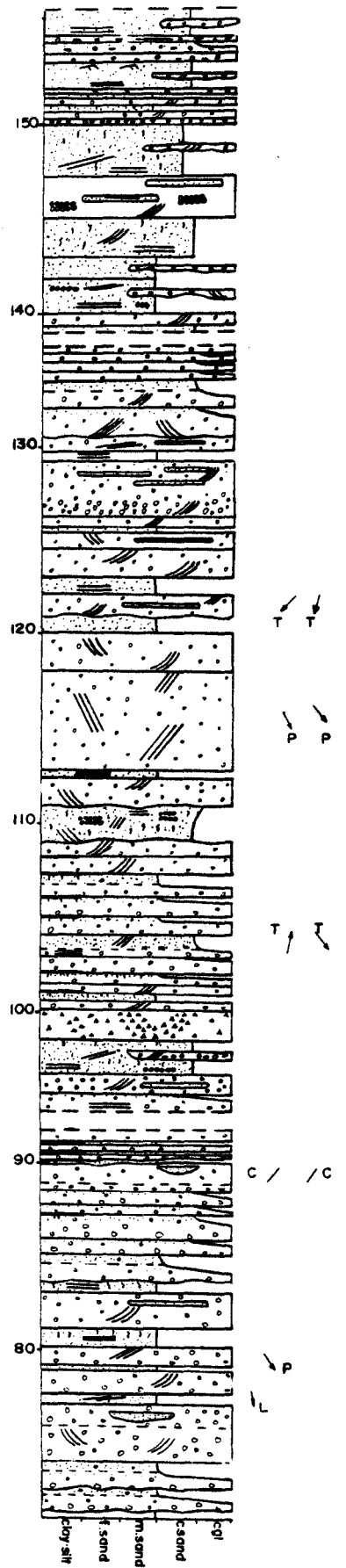
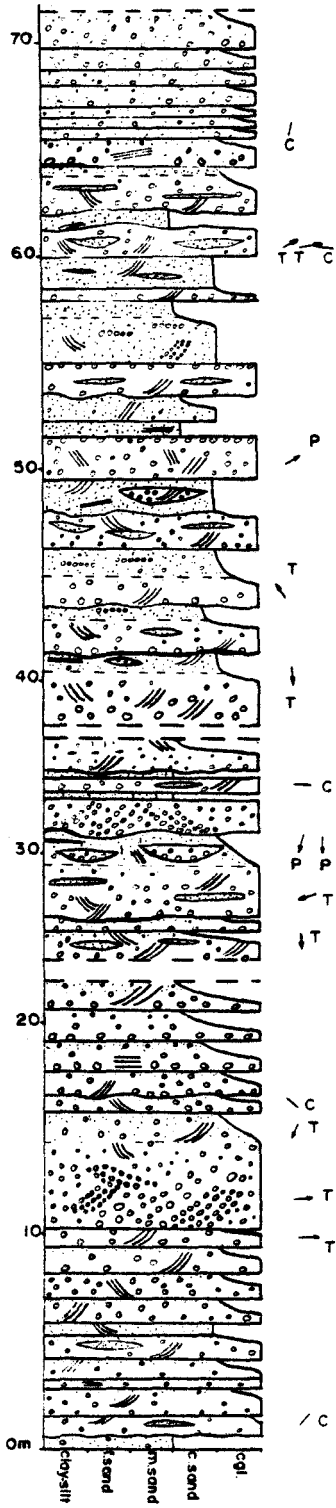
structure is planar-bedding with cross-bedding being rare. The bedding is considerably more continuous in nature and substantially thinner (Figure 2.1).

Figure 2.1 Detailed measured section. Note the increase in the amount of sandstones near the top and the abundance of cross-bedding.

Lepreau Fm.  
 Duck Cove Member  
 Duck Cove

Legend

- Planar tabular x-b P //
- Trough x-b T //
- Parallel bedding //
- Ripples ~
- Low-angle x-b L //
- Current lineation C //
- Burrows ~
- Mudclasts - - -
- Erosive ~
- Abrupt contacts -
- Gradational - - -



## Chapter 3

### Facies Description and Interpretation

#### 3.1 Introduction

Within a stratigraphic section, individual facies can be defined by field observations of its lithology, sedimentary structures, and organic aspects (Walker, 1979). The key to defining a facies classification is to be totally familiar with the rock body in question, a process that can be completed only after all field work has been done.

In the measured section, four main facies have been determined (Table 3.1), based primarily on gross grain size and are given a letter designation. Each facies is then subdivided into a subfacies with a numerical designation, a classification relying on the relative grain size and the difference in sedimentary structures.

#### 3.2 Facies Description

##### 3.2.1 Facies A

3.2.1.1 Introduction This facies is composed of conglomerates with various types and sizes of clasts which generally are rounded to well-rounded. The conglomerates are the dominant facies comprising roughly

Table 3.1

## Main Facies Types

---

Facies A	Conglomerates
Facies B	Sandstones
Facies C	Mudstones
Facies D	Breccias

---

55 % to 65% of the measured section. They are characteristically highly variable in grain size, matrix type, and sedimentary structures, and in lateral and vertical extent (Table 3.2). The conglomerates are red in colour although not as strongly hued as the sandstones. Some conglomerate beds have sharp, scoured bases and many have gradational tops.

3.2.1.2 Facies A<sub>1</sub> This facies is comprised of clast-supported conglomerates which characteristically occur in laterally lenticular beds.

This conglomerate occurs as rare 20 cm thick individual beds (Figure 3.1), or more commonly as local clast-supported lenses in channels. The clasts are rounded to well-rounded and range in size from 2 cm to 12 cm. The dominant lithology of the clasts is a grey-green aphanitic volcanic rock although quartzite clasts are also present. The nature of the matrix of both the individual beds and lenses is comprised of fine to medium sand.

The local clast-supported areas in channels are calcite cemented whereas, in the individual beds, cementation is not present (Figure 3,2).

Table 3.2

## Facies A

---

Facies A <sub>1</sub>	-	Clast-supported conglomerate, well rounded clasts.
Facies A <sub>2</sub>	-	Massive to planar-bedded conglomerate with substantial lateral and vertical variability.
Facies A <sub>3</sub>	-	Planar tabular cross-bedded conglomerate. Distinctive grey-green aphanitic volcanic clasts Calcite cement.
Facies A <sub>4</sub>	-	Conglomerate similar to A <sub>3</sub> , but with trough cross-bedding.

---

Figure 3.1 Clast-supported conglomerate of facies A<sub>1</sub>  
showing thin lenticular individual beds.  
Scale is 1 m.

Figure 3.2 Clast-supported conglomerate of facies A<sub>1</sub>.  
Note grey-green aphanitic volcanic clast type.  
Pen for scale is 15 cm long.



This facies is of relatively minor importance comprising less than 1-2% of the measured section.

3.2.1.3 Facies A<sub>2</sub> The conglomerates of this facies are matrix-supported, consisting of clasts of various sizes, shapes and types. The concentration of these clasts are extremely variable in extent both laterally and vertically. Rapid transitions between muddy matrix-supported and clast-supported, with clast size ranging from 1 cm to 12 cm, are not uncommon. In general this facies is the most variable of the conglomerates. Clasts average 3 cm in size and appear somewhat less rounded than in the other conglomerate facies.

The dominant sedimentary structure in this facies is planar bedding, although there is minor local cross-bedding. The bedding is usually defined by a concentration of clasts or as sandier laminae that have fewer pebbles. In many places, this facies is hard to distinguish from the sandstone facies B<sub>1</sub> and is gradational with it (Figure 3.3).

3.2.1.4 Facies A<sub>3</sub> The conglomerates of this facies are matrix-supported, consisting of clasts ranging

in size from 2 to 12 cm with an average of 6 cm. The clasts are rounded to well-rounded and consist of grey-green aphanitic volcanic rock, together with several types of granites and sedimentary rocks. The size fraction less than 2 cm in diameter is made up of angular quartz and feldspar fragments.

Calcite is very abundant as a cement or as stringer veins throughout the facies.

Individual beds are up to 1.5 m thick, commonly with a sharp base and a gradational upper contact with a sandstone facies. The dominant sedimentary structure is planar tabular cross-bedding, with the structure being defined by pebbles that lie on the foresets (Figure 3.4).

3.2.1.5. Facies A4 This facies is compositionally similar to that of facies A<sub>3</sub>, having many lithologies of clasts with the dominant grey-green aphanitic volcanic rock. This facies, however, tends to have higher concentrations of clasts which are rounded to well-rounded and range in size from 4 to 15 cm, averaging 9 cm (Figure 3.5).

The matrix is similar to the matrix of facies A<sub>3</sub>, comprising coarse angular fragments of quartz and

Figure 3.3 Planar-bedded matrix-supported conglomerate of facies A<sub>2</sub> filling a channel. Scale is 1m.

Figure 3.4 The planar-tabular cross-bedded conglomerate is at the top of the picture. Note the foresets defined by grain size change. Scale is 1 m.



Figure 3.5 Conglomerate is planar-bedded on the right side of the picture and trough cross-bedded filling a channel on the left side. Scale is 1 m.



feldspar. There is, however, more abundant calcite, both as cement and as stringer veins.

Individual beds range in thickness from 0.2 m to 1.5 m and are dominated by trough cross-bedding. The lower contact is invariably sharp and may show channels with a relief of up to 0.5 m. The upper contacts are erosional, abrupt or gradational into a sandstone facies.

### 3.2.2. Facies B

3.2.2.1 Introduction This facies consists of sandstones of various grain sizes, sedimentary structures and composition (Table 3.3). The sandstones are less laterally extensive than the conglomerates, primarily due to the scouring of the conglomerates. A general trend in the section is an increase in sandiness of the conglomerates and also an increase in the frequency and thickness of sandstone beds.

3.2.2.2. Facies B<sub>1</sub> This facies is defined as a pebbly coarse sandstone, similar in characteristics to the conglomerate facies A<sub>2</sub> except for a lower percentage of clasts (Figure 3.6).

Table 3.3

## Facies B

---

Facies B <sub>1</sub>	-	Massive to planar-bedded pebbly sandstone similar to facies A <sub>2</sub> .
Facies B <sub>2</sub>	-	Coarse pebbly sandstone which has planar tabular cross-bedding.
Facies B <sub>3</sub>	-	Coarse pebbly sandstone which has trough cross-bedding.
Facies B <sub>4</sub>	-	Medium-grained with well defined planar bedding.
Facies B <sub>5</sub>	-	Fine to medium-grained sandstone with low angle cross stratification.
Facies B <sub>6</sub>	-	Fine to medium-grained sandstone with ripples.

---

Sandstones of this facies invariably have gradational bases from a conglomerate, and may be laterally gradational with conglomerates of facies A<sub>2</sub>.

Sedimentary structures are not very well defined although stringers of pebbles may enhance the planar-bedding or trough cross-bedding. Locally the conglomerates can be clast-supported or, conversely, there can be many localized patches of planar-bedded medium-grained sandstones. These localizations of different grain size material and sedimentary structures are not distinctly different beds but rather are laterally and vertically gradational from the pebbly coarse sandstone.

3.2.2.3 Facies B<sub>2</sub> This facies is defined as a coarse sandstone with rare localized patches of clasts and medium-grained sandstones. The dominant sedimentary structures are planar tabular cross-bedding and planar bedding which are, in general, well defined.

The basal contact is in most cases gradational, whereas the top contact is sharply defined usually by an erosive conglomerate unit. The beds may reach a thickness of 1.5 m and a lateral extent of 20 m.

3.2.2.4 Facies B<sub>3</sub> This facies is very similar in characteristics to facies B<sub>2</sub> having localized patches of pebbles and medium-grained sandstone. Beds within this facies have gradational bases and sharp, erosive tops and are also of similar size and thickness to units within facies B<sub>2</sub>. The main difference is that the sandstones are trough cross-bedded to massive. Sandstones of this facies also have local patches of silts and fine sands.

3.2.2.5 Facies B<sub>4</sub> This facies is a red, medium sandstone that is characteristically planar bedded with very well defined laminae. The basal contact is quite sharp. The upper contact is also sharp primarily due to scouring before deposition of the succeeding conglomerate (Figure 3.7, 3.8).

The beds average 30 cm in thickness and are less than 5 m in lateral extent. This facies may be moderately burrowed although not extensively enough to obscure structure. Units of this facies may also be topped by mud drapes that are rippled.

Figure 3.6 Coarse pebbly sandstone of facies B<sub>1</sub> with indistinct bedding near the 1m scale.

Figure 3.7 Planar bedded sandstone of facies B<sub>4</sub> forming small pool deposits. Scale is 1m.



3.2.2.6 Facies B<sub>5</sub> This facies is defined as a medium to coarse sandstone with very well defined low angles cross-bedding (Figure 3.9). Both upper and lower contacts are sharp, the upper contact being erosional. Locally the foresets of the cross-beds have horizontal burrows in them (Figure 3.10).

Units of this facies range up to 10 m in lateral extent and reach 50 cm in thickness.

3.2.2.7 Facies B<sub>6</sub> This facies is a fine to medium-grained sandstone that occurs as very thin beds, usually less than 5 cm thick, and often with lenticular habit due to scouring of overlying conglomerate (Figure 3.11). This facies is found at the tops of a fining-upward cycles and may be overlain by mud drapes.

These sandstones have indistinct bedding although a few examples of current ripples can be found at the top. Some units appear to be extensively bioturbated as no structures were observed. Near the top of the section some of the sandstones lose the red colour and become distinctly grey in colour.

Figure 3.8 Planar bedded sandstone of facies B<sub>4</sub> with  
minor channel. Scale is 1m.

Figure 3.9 Medium-grained sandstone of facies B<sub>5</sub> with  
low angle cross stratification. Scale is 1m.

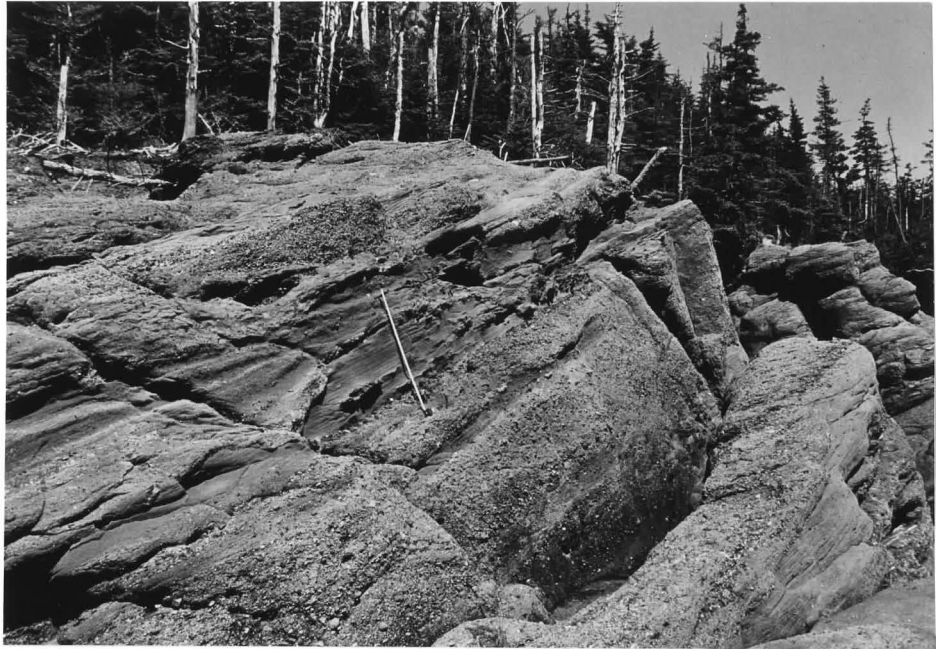


Figure 3.10 Burrowing on foresets of low angle cross  
beds of facies B<sub>5</sub>. Scale is 8 cm.

Figure 3.11 Fine-grained sandstone of facies B<sub>6</sub> with  
ripples and burrowing. Scale is 1m.



### 3.2.3. Facies C

This facies is described as a mudstone with strong red colouring (Figure 3.12). Mudstones may occur as extensively burrowed or rippled mud drapes over sandstones or as thin distinct beds. The beds average approximately 15 cm in thickness and 2 m in lateral extent. Laminae cannot be seen in the beds, probably due to extensive bioturbation. The beds have abundant grey-green bleach spots which are probably remnant root systems.

The contacts of these beds are sharp and well-defined, the top contact being erosional. By frequency and volume this is a minor facies of the measured section.

### 3.2.4 Facies D

This facies is also a minor component in the measured section where only one unit was found. This unit is a 0.5 m thick breccia with well-defined cross-bedding. The breccia differs from the conglomerate facies in that it has dominantly angular to sub-angular clasts a very muddy matrix. Clasts are granitic in lithology, and average 3 cm in size, although the largest observed clast measured 40 cm by 34 cm (Figure 3.13).

Figure 3.12 Mudstone bed of facies C filling a channel.  
Note ripples. Scale is 1m.

Figure 3.13 Cross-bedded breccia of facies D.  
Note the large clast. Scale is 1m.



### 3.3 Facies Interpretation

#### 3.3.1 Introduction

In evaluating a rock body, a key to the interpretation of a facies is to combine the observations of lithology and sedimentary structure, with an appreciation of the facies sequence or spatial relationship (Walker 1979). To test the relative validity of the interpretation, it is useful to compare it to well-studied stratigraphic units, as well as to observations of an analogous modern sedimentary environment.

Nadon (1981), in a brief study of the Lepreau Formation, determined that the Duck Cove Member is representative of a distal braided river like that of the Donjek type of Miall (1978), except deposited in a semi-arid environment. This conclusion was based on the lack of abundant clast-supported areas in the cross-bedded units, and also the lack of overbank deposits in association with the conglomerates. In addition, these deposits are spatially associated with the lower Fishing Point Member and the upper Maces Bay Member, which are interpreted to be debris flow deposits off a semi-arid alluvial fan.

The interpretation of each facies in this study will follow closely, the facies code and interpretation proposed by Miall (1978) for modern and ancient braided stream deposits and also to the facies code of Allen (1983).

### 3.3.2. Facies A

3.3.2.1 Facies A<sub>1</sub> This facies is described as a clast-supported conglomerate occurring as individual beds or as local concentrations in cross-bedded units. The individual beds are probably the result of lag deposits of flows of upper flow regime decreasing in velocity. The local concentration usually occur at the base of erosional trough cross-bedded units and can be up to 15 cm in length. These pebbles were also deposited when the fluid slowed and the flow was no longer capable of carrying them as bed load.

3.3.2.2 Facies A<sub>2</sub> This facies is a matrix-supported conglomerate that may be massive but predominately contains crudely defined planar bedding. This facies in conjunction with facies B<sub>1</sub>, shows the greatest lateral and vertical variability. Facies A<sub>2</sub> corresponds

to facies Gm of Miall (1978), which he interprets as being longitudinal bars or lag sieve deposits. Allen (1983) classifies this facies as G<sub>2</sub> and finds that it occurs in plane-bedded simple bars or as tops of compound or composite-compound bars.

3.3.2.3 Facies A<sub>3</sub> This facies is also a matrix-supported conglomerate, but with dominantly planar tabular cross-bedding. It corresponds to facies Gp of Miall (1978), which he interprets as representing linguoid bars or as deltaic growths from older bar remnants. Allen (1983) classifies this facies as G<sub>3</sub>, and finds it is the primary structure in cross-bedded simple bars. In the compound and composite-compound bars, the sediment is deposited on the stoss-side of the bar producing planar lamination of facies G<sub>2</sub>, which then avalanches down producing facies G<sub>3</sub>. Other terms used in the literature for describing bars composed of this facies are transverse, slipface or cross-channel.

3.3.2.4 Facies A<sub>4</sub> This is a matrix-supported conglomerates with dominantly trough cross-bedding. This

facies corresponds to facies Gt of Miall (1978) and is considered to represent in-channel deposition. Allen (1983) did not recognize this facies in his study.

### 3.3.3 Facies B

3.3.3.1 Facies B<sub>1</sub> Except for a decrease in the amount of pebble-size fraction, this facies has the same characteristics as facies A<sub>2</sub>. Therefore, it may be also interpreted as a longitudinal bar, which corresponds to facies Gm of Miall (1978) and to facies G<sub>2</sub> of Allen (1983).

3.3.3.2 Facies B<sub>2</sub> This facies is a coarse pebbly sandstone with planar tabular cross-bedding and is recognized as facies Sp of Miall (1978) and facies S, of Allen (1983). Units of this facies have been interpreted to represent linguoid or transverse bars, or sandwaves of the lower flow regime.

3.3.3.3 Facies B<sub>3</sub> This facies is a coarse-grained, pebbly sandstone with trough cross-beds and is recognized as facies St of Miall (1978) and facies S<sub>3</sub> of Allen (1983). The trough cross-bedding is the result

of deposition of sinuous crested dunes in a lower flow regime.

3.3.3.4 Facies B<sub>4</sub> This facies is a medium-grained sandstone which has distinctive well-defined planar laminations and is recognized as facies Sh of Miall (1978) and facies S<sub>4</sub> or S<sub>5</sub> of Allen (1983). The planar bedding is the result of planar flow in the upper flow regime.

3.3.3.5 Facies B<sub>5</sub> This facies is fine to medium-grained sandstone which has low angle cross-bedding and is recognized as facies S1 of Miall (1978) and facies S<sub>5</sub> of Allen (1983). The low angle cross-bedding is the result of shallow, high velocity flow into low relief scours (Rust 1978).

3.3.3.6 Facies B<sub>6</sub> This facies is a fine to medium-grained sandstone with abundant ripples, and is recognized by Miall (1978) as facies Sr. The ripples are representative of lower flow regime.

#### 3.3.4 Facies C

This facies occurs as finely laminated mudstones or as mud drapes, which may be rippled. It is equivalent to facies F1 or Fm of Miall (1978) and to facies M of Allen (1983). The finely laminated mudstone is interpreted as representing overbank deposits, whereas the mud drapes represent a waning flood deposit.

#### 3.3.5 Facies D

This facies is defined as a breccia because of the sub-angular to angular nature of its clasts. Facies D has poorly defined cross-bedding and is equivalent to facies Gt or Gp of Miall (1978) and facies G<sub>3</sub> of Allen (1983). The facies might indicate the reworking of a debris flow.

A summary of the facies codes are given in Table 3.4.

### 3.4 Summary

#### 3.4.1 Introduction

A discussion of facies descriptions and interpretations of a given measured section is incomplete with-

Table 3.4

## Summary of Facies Code

---

Loosemore	Miall (1978)	Allen (1983)
A <sub>1</sub>	-	-
A <sub>2</sub>	Gm	G <sub>2</sub>
A <sub>3</sub>	Gp	G <sub>3</sub>
A <sub>4</sub>	Gt	-
B <sub>1</sub>	Gm	G <sub>3</sub>
B <sub>2</sub>	Sp	S <sub>1</sub>
B <sub>3</sub>	St	S <sub>3</sub>
B <sub>4</sub>	Sh	S <sub>4</sub> , S <sub>5</sub>
B <sub>5</sub>	Sl	S <sub>5</sub>
B <sub>6</sub>	Sr	-
C	Fm, Fl	M
D	Gt, Gp	G <sub>3</sub>

---

out an idea of the vertical succession of these facies. This study uses the statistical method of the Markov chain analysis and observations of facies assemblages in other braided stream deposits.

#### 3.4.2 Markov Chain Analysis

The Markov chain analysis is a statistical approach to determine the probability of one facies being succeeded by another facies. The probability could be defined as the relative frequency in the total population of transitions from which the sample was drawn.

In order to simplify the analysis, the minor facies have been incorporated into the major facies. Therefore facies B<sub>1</sub>, because of its similar characteristics can be considered under facies A<sub>2</sub>. The one unit of facies D is considered to belong to facies A<sub>4</sub> and facies B<sub>5</sub> is considered to belong to facies B<sub>4</sub>. In addition a scour surface indicated by SS has been incorporated into the analysis.

The analysis used in this study is a first order Markov chain (Miall 1973) which considers the relationship between a given bed and the next bed immediately above it.

This method, however, does not consider the thicknesses of the beds nor does it account for the transition of a bed of one facies to another bed of the same facies.

The first step in a Markov analysis is to set up a transition count matrix which is designated  $T_{ij}$ . This matrix, given in Appendix A1 , is a two-dimensional array which tabulates the number of times all possible vertical facies transitions occur in the measured section. For example, facies A<sub>2</sub> is succeeded by facies B<sub>2</sub>, 15 times.

From the transition count matrix, two probability matrices is derived. The first, given the designation  $P_{ij}$  and tabulated in Appendix A2 , represents the actual probability of the given facies transitions occurring in the measured section. For example, the transition of A<sub>2</sub> to B<sub>2</sub> occurs 15 times out of all 39 transitions from A<sub>2</sub> and therefore the probability of transition is  $15/39=0.385$ .

The second probability matrix given the designation  $R_{ij}$  (Appendix A3 ), represents the probability of the given facies transition occurring randomly. For the example of the transition from A<sub>2</sub> to B<sub>2</sub>, the total number of transitions of any facies to B<sub>2</sub> is 36. The total of transitions possible to a given facies but not itself, is the grand total number

of transitions (193) minus the number of transitions to facies A<sub>2</sub> (39). Therefore the random probability of transition from facies A<sub>2</sub> to facies B<sub>2</sub> is  $36/(193-39)=0.234$ .

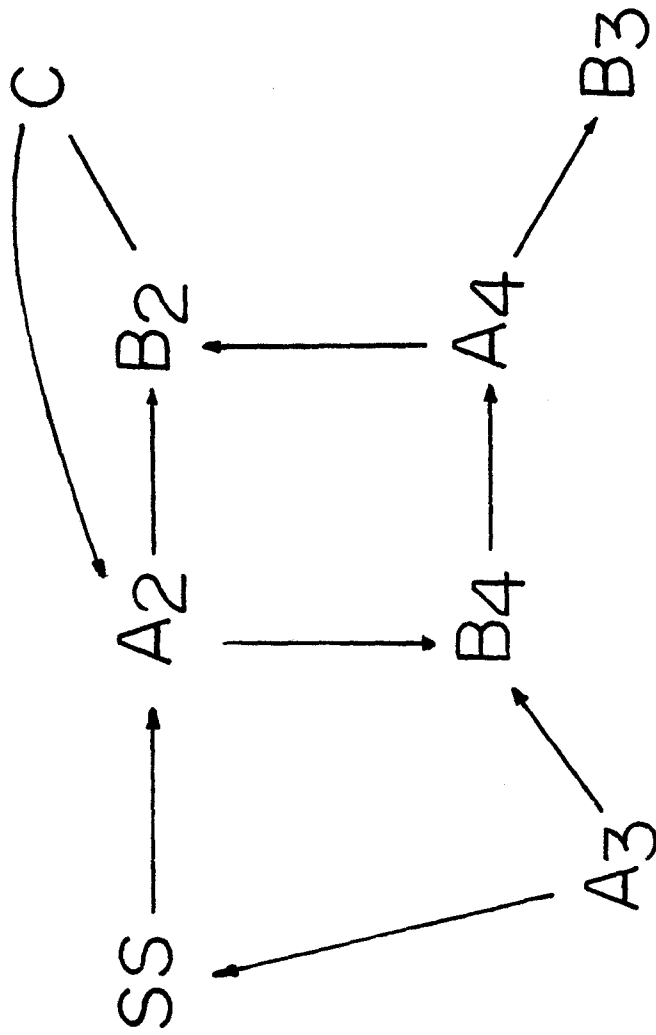
To compare the actual observed probabilities to the random probabilities, a new matrix is determined as the actual minus the random probabilities. The matrix is called the difference matrix and is designated as  $D_{ij}$  (Appendix A4) where  $D_{ij} = P_{ij} - R_{ij}$ . For the example from facies A<sub>2</sub> to B<sub>2</sub>,  $D(1,4) = 0.385 - 0.234 = 0.151$ .

From the difference matrix a preferred facies relationship diagram can be constructed (Walker, 1979). A simplified version of this diagram is give in Figure 3.14 . This figure suggests five different sequences which are listed below.

- (i) SS -- A<sub>2</sub> -- B<sub>2</sub> -- C
- (ii) SS -- A<sub>2</sub> -- B<sub>4</sub>
- (iii) A<sub>4</sub> -- B<sub>2</sub> -- C
- (iv) A<sub>4</sub> -- B<sub>3</sub>
- (v) A<sub>3</sub> -- B<sub>4</sub>

Sequence (i) suggests migration of a longitudinal bar over a channel floor, succeeded by a linooid bar with waning flow mud drapes. The sequence may repeat with the

Figure 3.14 Preferred facies relationship diagram for  
the measured section.



formation of a new longitudinal bar.

Sequence (ii) also suggests migration of a longitudinal bar which is succeeded by planar bedded sandstone.

Sequence (iii) is only slightly more common than random probability predicts. It represents channel-fill, succeeded by growth of a linguoid bar into the channel.

Sequence (iv) represents channel fill followed by the formation of sinuous crested dunes.

Sequence (v) probably represents the formation of either a compound or composite-compound bar of Allen (1983).

It is necessary to determine whether or not the observed probabilities differ from the random probabilities simply by sampling variability. With a 5% level of significance and one degree of freedom, the Chi square value is 3.84. Where the Chi square is:

$$x^2 = \frac{(\text{observed freq} - \text{predicted freq})^2}{\text{predicted freq}}$$

This is tabulated in Appendix A5 .

For the example of the transition of facies A2 to B2, the Chi square value is 3.78, or slightly below the value of 3.84. This suggests that the null hypothesis must be accepted, where the null hypothesis states that the results could be achieved by random sampling of a

uniform distribution.

However for the purposes of this study this value is considered to be almost significant and therefore not rejected as random. The significant and almost significant transitions are listed in Table 3.5.

### 3.4.3 Facies Assemblages

The Markov chain analysis has suggested 5 succession cycles which, when applied to the vertical sequence, can help interpret the measured section. These succession cycles are imposed on the stratigraphy in Figure 3.15.

This figure shows predominantly channel fill succession at the base of the section, which corresponds to the thick coarse nature of the beds. This is succeeded by the growth of compound or composite-compound bars of Allen (1983), which are accompanied by minor channel fill. Near the top, these bars are succeeded by the growth of longitudinal bars, again with minor channel fills.

These observations, in combination with an upward decrease in grain size and thickness of beds, suggest an increase in the relative distance from the source. The area is assumed to be semi-arid (Nadon, 1981) and an

Table 3.5

## Significant and Almost Significant Transitions

---

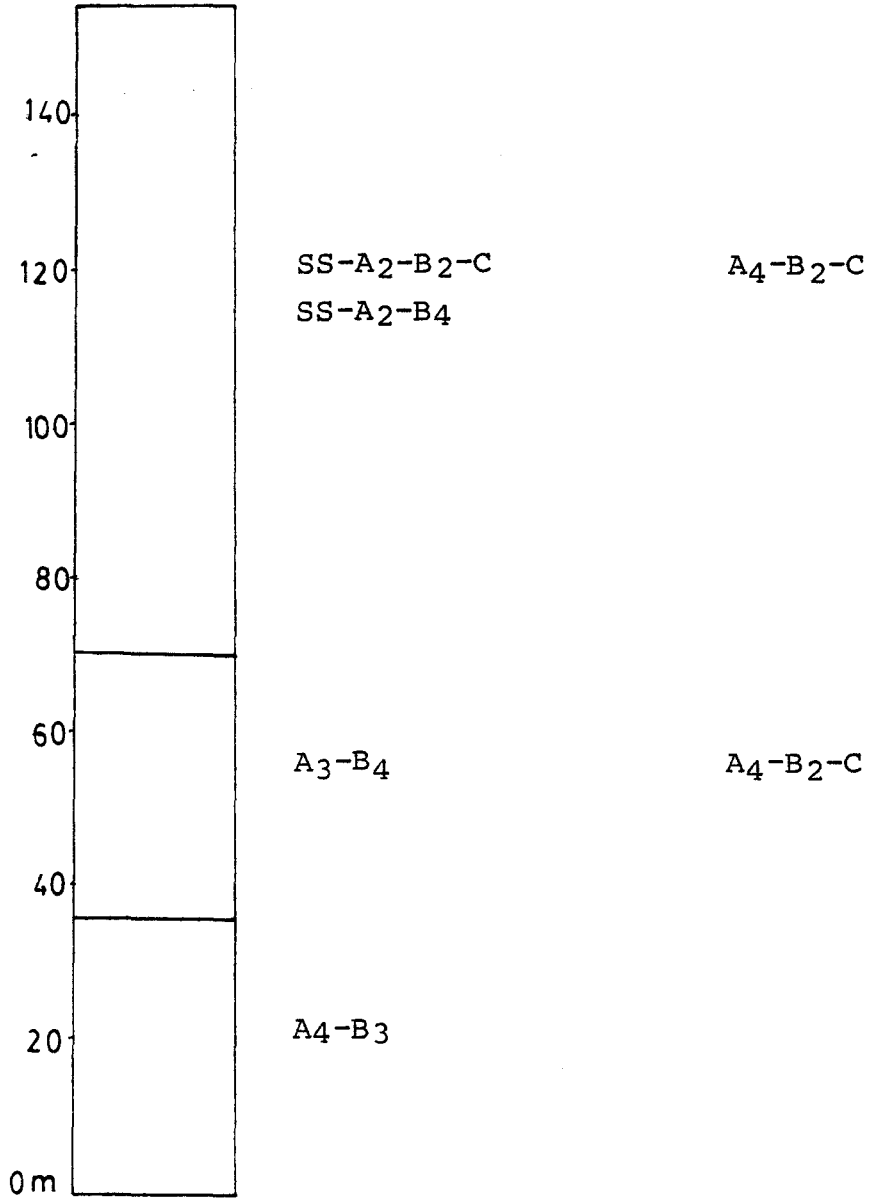
Significant	Almost Significant
SS-A <sub>2</sub>	A <sub>2</sub> -B <sub>2</sub>
B <sub>2</sub> -C	B <sub>3</sub> -A <sub>4</sub>
A <sub>4</sub> -A <sub>4</sub>	

---

Figure 3.15 Succession Cycles determined from the Markov chain analysis imposed on the stratigraphy of the measured section.

Major Succession

Minor Succession



increase in aridity, which would reflect in a decrease in discharge, might produce this succession of facies.

Vertical profiles have been constructed by Miall (1978) to represent the different types of braided stream deposits. The measured section fits numerically into the Donjek type because it consists of 55 to 65% conglomerates. The Donjek type is considered to represent distal gravelly rivers with cyclic-type deposits (Miall 1978, Rust 1978). A comparison of the facies assemblages of the Donjek type to the measured section is give in Table 3.6 using the facies code after Miall (1978).

Because there are only slight differences between the two sections, the measured section can be considered to be of the Donjek type. This conclusion is justified, even though the two sections were deposited in different climatic zones, because the flashy discharge and ratio of sand to gravel are the actual controls on bar formation (Bluck, 1979). The climatic effect is only reflected in the vertical accretion deposits which are rarely preserved in the rock record.

Table 3.6

## Facies Assemblages

	Main facies	Minor facies
Donjek type	Gm, Gt, St	Gp, Sh, Sr, Sp, Fl, Fm
Measured section	Gm, Gt, Sh Sp	Gp, St, Sl, Fl, Fm, Sr

## Chapter 4

### Paleocurrent

#### 4.1 Introduction

Although exposure of the measured section is adequate and flow indicators such as cross-bedding are abundant, the amount of paleocurrent data is relatively meager. This lack of data is primarily due to the faulting and jointing of the cliffs, which produce outcrops that tend to have smooth, flush faces. This fact makes the obtaining of paleocurrent data from cross-beds difficult and often unreliable.

The nature of the cross-beds foresets also contribute to the difficulty in obtaining reliable data. The cross-beds foresets are of two types as recognized by Eynon (1972): an openwork gravel type and a heterogeneous gravel type. The open-work gravel type consists of a clast-rich foreset base and bed base which grade outwards and upwards. The heterogeneous gravel type have foresets defined only by a subtle change in grain size. At a distance these foresets can be recognized by strings of pebbles but identification becomes difficult when the observer moves close to the outcrop to measure the

orientation of the structure.

Another difficulty encountered was an inability, in some instances, to determine whether the cross-beds were trough cross-beds or planar cross-beds. Some structures appear to be planar cross-beds but had very well-defined asymptotic toes. This may have been a reflection of either the shape of outcrop or alternatively, a transitional state between trough cross-beds and planar cross-beds in the depositional environment.

#### 4.2 Method

Measurements were taken from three types of sedimentary structures: current lineation, planar cross-beds and trough cross-beds. The measurements were then rotated by using a stereonet to correct for tectonic dip which averages about 30 towards the northeast in the section.

The corrected data was then plotted on rose diagrams using the method proposed by Curray (1956). In this method, the vector mean, vector strength or magnitude and amount of dispersion are calculated.

The rose diagrams are plotted using the square root of the percentage of readings. This method is

employed because the area of the piece of the pie is proportional to the square of the number of readings. The result would be similar by plotting the percentage of the number of readings but the area of the pie would not correspond correctly to the number of readings.

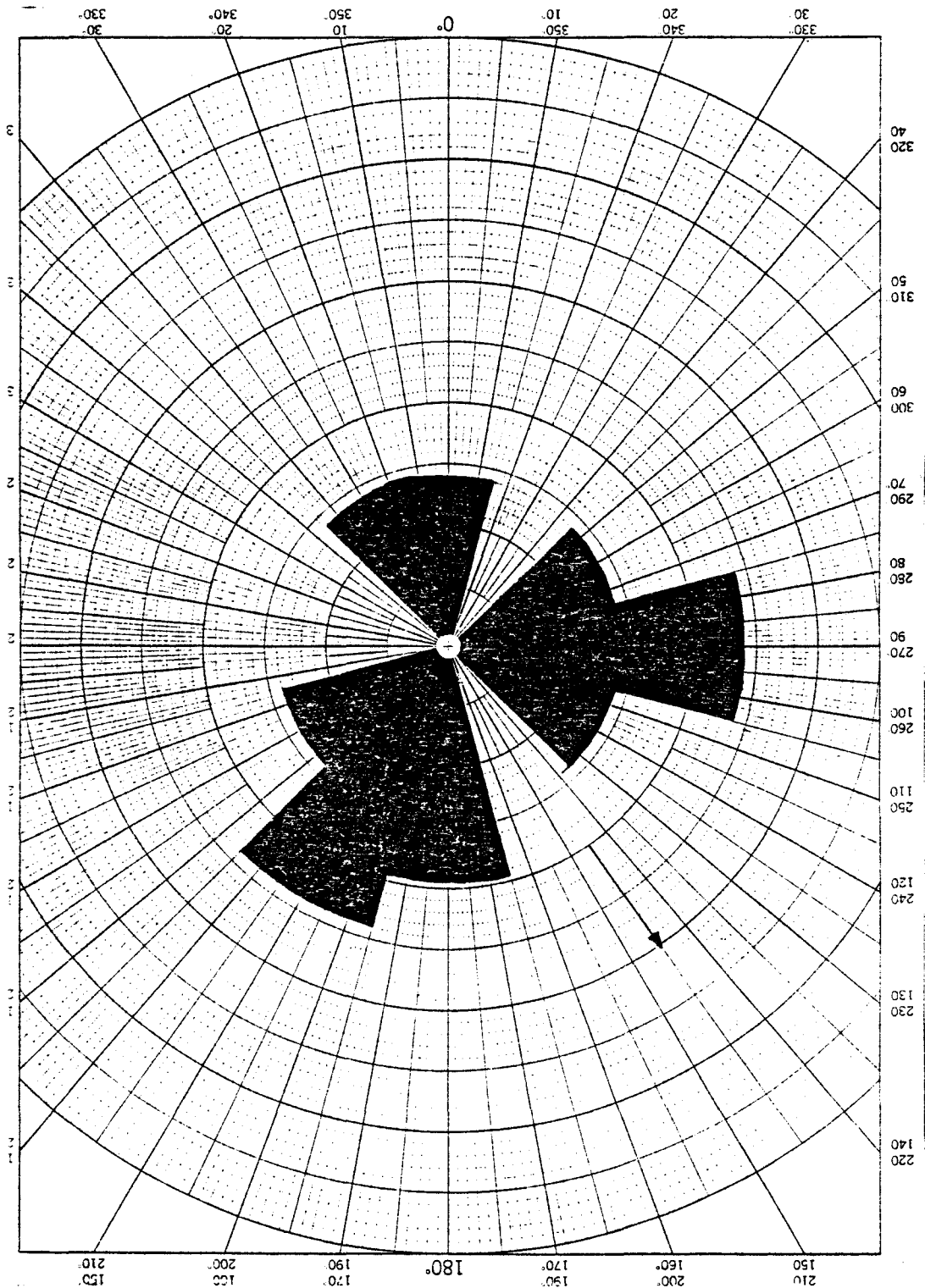
A test of the null hypothesis was conducted by using the Rayleigh method. This test determines if the result was random sampling with uniform distribution.

#### 4.3 Results

The measurement of trough cross-beds in the section with  $n=13$ , reveals a mean of  $145^\circ$  ( $L=28\%$ ) (Appendix B1 ) and these cross-beds are plotted on a rose diagram in Figure 4.1. The results show essentially a bimodal distribution to the east and south in addition to a spurious mode to the north-northwest. An examination of modern braided gravelly rivers by Williams and Rust (1969), suggests that trough cross-beds are not always an accurate indicator of mean flow because the cross-beds often form at a very high angle to the mean direction of flow.

The measurement of planar cross-beds in the section

Figure 4.1 Rose diagram plot for trough cross-beds  
n=13, L=28%, vector mean = 145°



with  $n=6$ , reveals a mean of  $152^\circ$  ( $L=12\%$ ) (Appendix B2) and these cross-beds are plotted on a rose diagram in Figure 4.2. The results show a slight bimodal appearance although with only six measurements, this is not a statistically correct observation.

Williams and Rust (1969) suggest that to obtain good reliable results, it is best to use small-scale structures such as ripples or current lineations.

The current lineations are small channels or grooves and since they are bidirectional, they imply only an orientation of flow. A calculation of a grand mean for all cross-bedding with  $n=13$ , reveals a value of  $146^\circ$  ( $L=23\%$ ) (Appendix B3). Therefore assuming that the overall flow is to the south, a weighting of the current lineation to the south reveals a vector mean with  $n=6$  of  $184^\circ$  ( $L=11\%$ ). The rose diagram with weighting to the south is plotted in Figure 4.3.

A grand mean calculated from all three sedimentary structures gives a value of  $151^\circ$  where  $n=25$  and  $L=20\%$ .

Work on the Platte River (Smith 1972) reveals that with both active and exposed bars, the vector mean

Figure 4.2 Rose diagram plot for planar tabular cross-  
beds  $n=6$ ,  $L=12\%$ , vector mean =  $152^\circ$

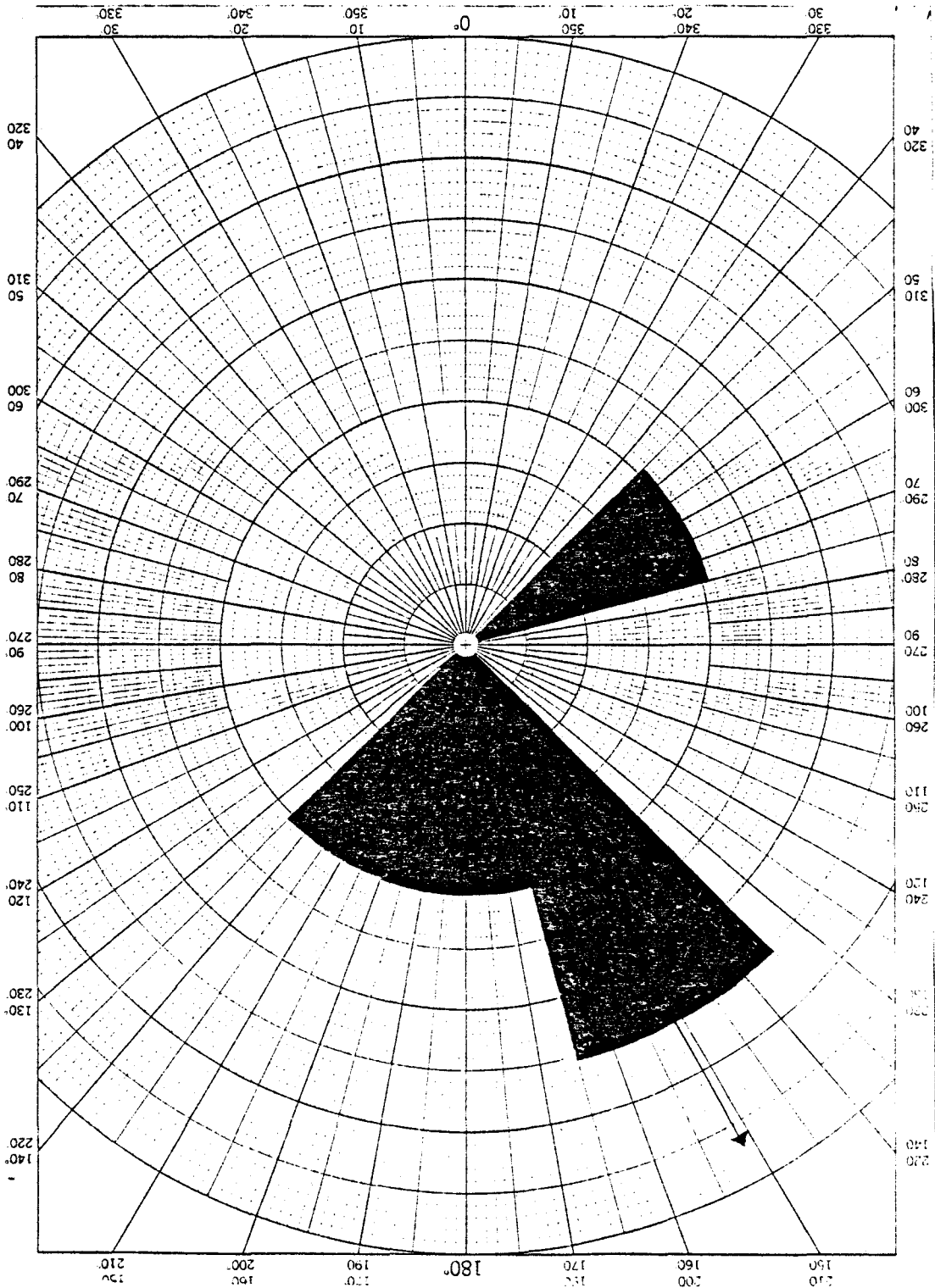
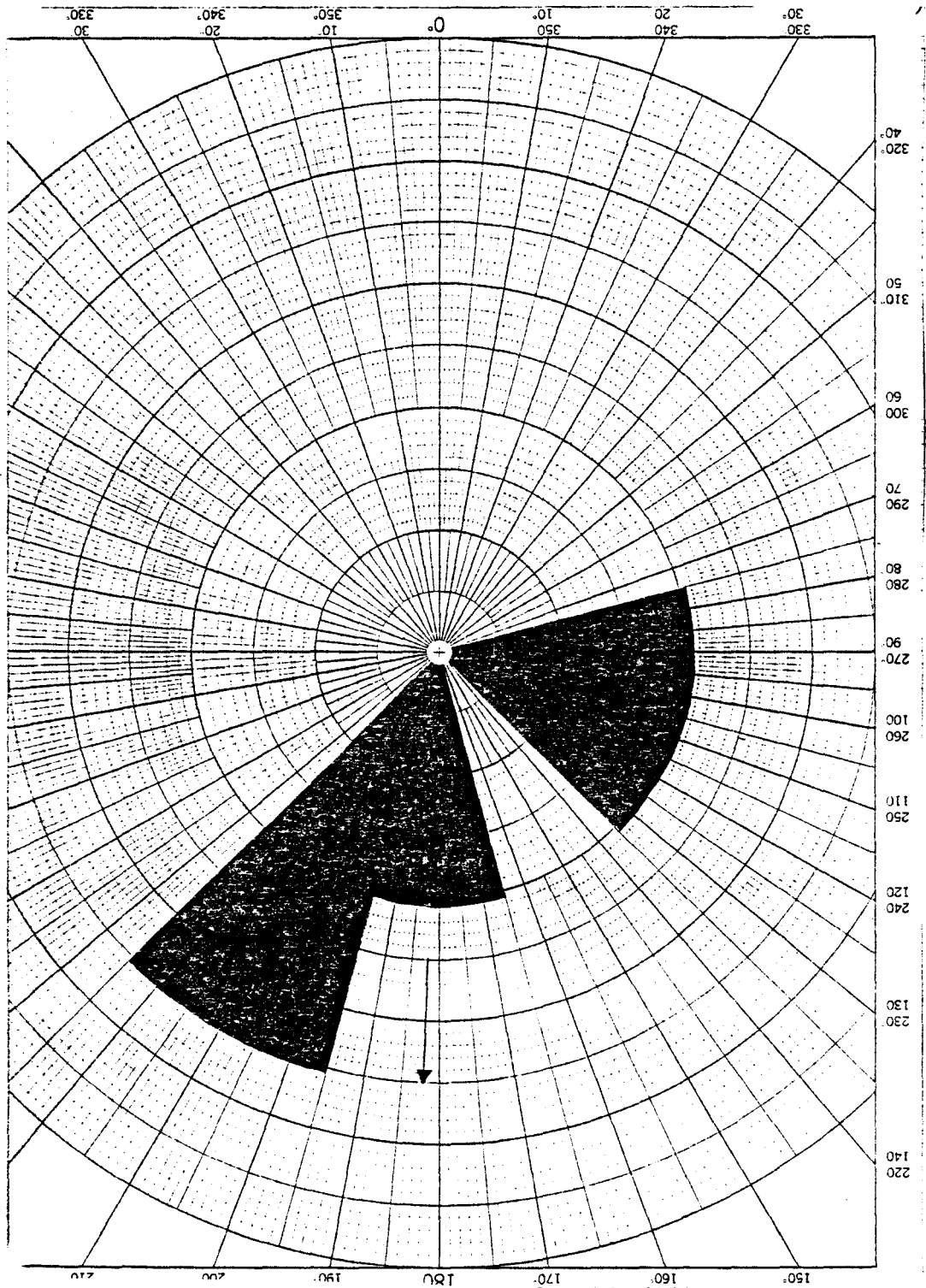


Figure 4.3 Rose diagram plot for current lineations

n=6, L=11%, vector mean = 184°



of planar cross-beds correspond closely to the trend of the main channel although the dispersion is considerable. For low flood stage the variance is reported to be 3965 on active bars and 5650 on exposed bars. The variance is simply the square of the standard deviation which can be determined by using the method of Curry (1956).

Potter and Pettijohn (1963) report a general range of variance between 4000 and 6000 for fluvial-deltaic deposits. However, Banks and Collinson (1973) suggest that the calculation of variance on modern deposits leads to an overestimated value when compared to the value for ancient braided deposits. This overestimation may result because the lowest variance occurs in the portion of the bar that is most likely to be preserved. Williams and Rust (1969) report a standard deviation about the vector mean of  $20^{\circ}$  -  $30^{\circ}$  or a variance of less than 1000 for the gravelly braided Donjek River.

Calculations for planar cross-bedded units in this study reveal a standard deviation of 48 or a variance of approximately 2300. This would compare roughly with that of the Donjek River. The difference in variance is due to the complexities of each individual depositional

environment. Grain size and climatic differences would be expected to influence the sedimentary structures, thereby affecting the variance.

The value determined in this study for trough cross-beds is  $77^\circ$  for standard deviation and 5929 for variance. For current lineation the standard deviation is  $49^\circ$  or a variance of about 2400. Such a large variance value for trough cross-beds appear to support the need to use small-scale structures to determine an accurate paleoflow indication.

## Chapter 5

## Conclusions

The main contribution of this study is the detailed description of the facies and the facies succession, which complement the conclusion of Nadon (1981) that this member can be interpreted as a distal braided river of the Donjek type (Miall 1978).

This conclusion stands despite the Donjek River being deposited in a humid climatic environment, while the braided river forming the measured section was deposited in a semi-arid environment. A better modern analogue needs to be recognized for a semi-arid braided river system.

References

- Alcock, F. J., 1945, Preliminary map, Musquash New Brunswick: Geol. Survey of Canada Paper 45-2
- Allen, J. R. L., 1983, Studies in Fluvatile sedimentation: bars, bar-complexes and sandstone sheets (low sinosity braided streams) in the Brownstones (L. Devonian), Welsh Borders, Sediment Geol., v.33, p.237-293
- Bailey, L. V., and Matthews, G. F., 1872, Preliminary report on the geology of southern New Brunswick: Geol. Survey of Canada, Rept. of Progress, p. 13-240
- Banks, N. L., and Collinson, J. D., 1973, Some sedimentological aspects of planar cross-stratification in a sandy braided river: Jour. Sed. Petrology v. 42(3) p. 265-267
- Belyea, H. R., 1939, The geology of Musquash, New Brunswick (Ph. D. thesis): Evanston, Il. Northwestern Univ., 109 p.
- Bluck, B. J., 1979, Structure and directional properties of some valley sandur deposits in Southern Iceland: Sediment., v. 21(4) p. 533-554

- Curray, J. R., 1956, Analysis of two-dimensional  
orientation data: Jour. Geol., v. 64, p. 117-131
- Eynon, G., 1972, The structure of braid bars: Facies  
relationship of pleistocene braided outwash  
deposits, Paris, Ont. (Ms c. Thesis):  
Hamilton, Ont., McMaster Univ.
- Klein, G. de V., 1962, Triassic sedimentation,  
Maritime Provinces, Canada: Geol. Soc.  
America Bull., v. 73, p. 1127-1146
- \_\_\_\_\_, 1963, Regional implications of Triassic  
paleocurrents, Maritime Provinces, Canada:  
Jour. Geol., v. 71, p. 801-808
- Le Pichon, X., and Fox, P. J., 1971, Marginal Offsets,  
fracture zones and the early opening of the  
North Atlantic: Jour. Geophys. Res., v. 76,  
p. 6294-6308
- Matthews, G. F., 1896, Report on the Summer Camp of 1895:  
N. B. Nat. History Soc. Bull., v. 16, p. 67-72
- Miall, A. D., 1973, Markov chain analysis applied to an  
ancient alluvial plain sequence sediment,  
v. 20, p. 347-364
- \_\_\_\_\_, 1978, Lithofacies and vertical profile

- models in braided river deposits: A summary,  
in Miall, A. D., ed., *Fluvial Sedimentology*:  
Canadian Soc. Petrol. Geol. Memoir 5, p. 597-604
- Nadon, G. S., 1981, *The stratigraphy and sedimentology of  
the Triassic at St. Martins and Lepreau,  
New Brunswick. (MSc. Thesis)*  
Hamilton, Ont., McMaster Univ.
- Potter, P. E., and Pettijohn, F. J., 1963, *Paleocurrents  
and Basin Analysis*: Springer-Verlag, 296 p
- Rust, B. R., 1978, *Depositional models for braided alluvium  
in Miall, A. D., ed, Fluvial Sedimentology,  
Canadian Soc. Petro. Geol. Memoir 5, p. 605-626*
- Rust, I., *Unpublished field notes of the Lepreau For-  
mation, New Brunswick*
- Sargeant, W. A., and Stringer, P., 1977, *Triassic reptile  
tracks in the Lepreau Formation, southern New  
Brunswick, Canada: Can. Jour. Earth Sci.,  
v. 15, p. 594-602*
- Smith, N. D., 1972, *Some sedimentological aspects of planar  
cross-stratification in a sandy braided river:  
Jour. Sed. Petro., v. 42(3), p. 624-626*
- Swift, D. J. P., and Lyall, A. K., 1968, *Origin of the*

Bay of Fundy, an interpretation from sub-bottom profiles: Marine Geol., v. 6, p. 331-343

Walker, R. G., 1979, Facies and facies models. General introduction, sandy fluvial systems in Walker, R. G., ed., Facies Models, Geo science Canada reprint series 1: Kitchener, Ainsworth Press p. 1-8, 23-31

Williams, P. F., and Rust, B. R., 1969, The sedimentology of a braided river: Jour. Sed. Petrol., v. 39, p. 649-679

Wright, W. J., and Clements, C. S., 1943, Coal deposits of Lepreau-Musquash district, New Brunswick: Acadian Nat., v. 1, p. 5-27

## Appendix A1

## Transition Matrix

	A <sub>2</sub>	A <sub>3</sub>	A <sub>4</sub>	B <sub>2</sub>	B <sub>3</sub>	B <sub>4</sub>	C	SS	
A <sub>2</sub>	0	2	6	15	2	13	0	1	39
A <sub>3</sub>	2	0	1	2	0	4	0	2	11
A <sub>4</sub>	6	2	0	13	9	9	0	2	41
B <sub>2</sub>	10	1	10	0	2	2	7	4	36
B <sub>3</sub>	0	2	7	2	0	0	0	3	15
B <sub>4</sub>	7	3	11	2	1	0	1	3	28
C	6	0	2	0	0	0	0	0	8
SS	7	1	4	2	0	1	0	0	15
	38	11	41	36	14	29	8	14	193

## Appendix A2

## Actual Probability Matrix

0	0.051	0.154	0.385	0.051	0.333	0	0.026
0.182	0	0.091	0.182	0	0.364	0	0.182
0.146	0.049	0	0.317	0.220	0.220	0	0.049
0.278	0.028	0.278	0	0.056	0.056	0.194	0.111
0	0.133	0.467	0.133	0	0	0	0.120
0.250	0.107	0.393	0.071	0.036	0	0.036	0.107
0.750	0	0.250	0	0	0	0	0
0.467	0.067	0.267	0.133	0	0.067	0	0

## Appendix A3

## Random Probability Matrix

0	0.071	0.266	0.234	0.091	0.188	0.052	0.091
0.209	0	0.225	0.198	0.078	0.159	0.044	0.078
0.208	0.072	0	0.237	0.092	0.191	0.053	0.092
0.242	0.070	0.261	0	0.089	0.185	0.051	0.089
0.213	0.062	0.230	0.202	0	0.163	0.045	0.079
0.230	0.067	0.248	0.218	0.085	0	0.048	0.085
0.205	0.059	0.222	0.195	0.076	0.151	0	0.076
0.213	0.062	0.230	0.202	0.079	0.163	0.045	0

Appendix A4

Difference Matrix

0	-0.020	-0.112	0.151	-0.040	0.145	-0.052	-0.065
-0.027	0	-0.134	-0.016	-0.078	0.205	-0.044	0.104
-0.062	-0.023	0	0.086	0.128	0.029	-0.053	-0.043
0.036	-0.042	0.017	0	-0.033	-0.129	0.143	0.022
-0.213	0.071	0.287	-0.069	0	-0.163	-0.045	0.035
0.020	0.040	0.145	-0.147	-0.049	0	-0.012	0.022
0.545	-0.059	0.028	-0.195	-0.076	-0.151	0	-0.076
0.254	0.005	0.037	-0.069	-0.079	-0.096	-0.045	0

## Appendix A5

## Chi Square Matrix

0	-	-	3.78	-	0.77	-	-
-	0	-	-	-	2.89	-	1.52
-	-	0	1.11	7.25	0.17	-	-
0.19	-	0.04	0	-	-	14.52	0.20
-	1.23	3.65	-	0	-	-	2.86
0.05	0.67	2.37	-	-	0	-	0.16
11.59	-	0.03	-	-	-	0	-
4.53	0.01	0.09	-	-	-	-	0

## Appendix B1

## Trough Cross-Beds

$\theta$	n	%	$\sqrt{\%}$
345-15	1	7.7	2.8
045-075	1	7.7	2.8
075-105	3	23.1	4.8
105-135	1	7.7	2.8
165-195	2	15.4	3.9
195-225	3	23.1	4.8
225-255	1	7.7	2.8
315-345	1	7.7	2.8

$$V = -3.009$$

$$W = 2.084$$

$$\theta = 145^\circ$$

$$R = 3.66$$

$$L = 28\%$$

$$S = 77^\circ$$

$$\text{variance} = 5929$$

$$\text{Rayleigh test} = 1 - e^{-\left(\frac{R^2}{N}\right)}$$

$$= 0.65$$

$\therefore$  reject null hypothesis  
( $>0.05$ )

## Appendix B2

## Planar Cross-Beds

$\theta$	n	%	$\sqrt{\%}$
045-075	1	16.6	4.1
135-165	3	50.0	7.1
165-195	1	16.6	4.1
195-225	1	16.6	4.1

$$V = -0.655$$

$$W = 0.355$$

$$\theta = 152^\circ$$

$$R = 0.745$$

$$L = 12\%$$

$$S = 48^\circ$$

$$\text{variance} = 2304$$

$$\text{Rayleigh test} = 1 - e^{-\left(\frac{R^2}{N}\right)}$$

$$= 0.09$$

∴ reject null hypothesis  
( $>0.05$ )

## Appendix B3

Current Lineation (with assumed southerly direction)

$\theta$	n	%	$\sqrt{\%}$
075-105	1	16.6	4.1
105-135	1	16.6	4.1
165-195	1	16.6	4.1
195-225	3	50.0	7.1

V=-0.670

W=-0.049

 $\theta=184^\circ$ 

R=0.672

L=11%

S=49°

variance = 2401

Rayleigh test =  $1 - e^{-\frac{A^2}{N}}$   
 = 0.07

∴ reject null hypothesis  
 (>0.05)